

# INTERNATIONAL SOCIETY FOR SOIL MECHANICS AND GEOTECHNICAL ENGINEERING



*This paper was downloaded from the Online Library of the International Society for Soil Mechanics and Geotechnical Engineering (ISSMGE). The library is available here:*

<https://www.issmge.org/publications/online-library>

*This is an open-access database that archives thousands of papers published under the Auspices of the ISSMGE and maintained by the Innovation and Development Committee of ISSMGE.*

## Groundwater drawdown induced ground settlement during tunneling – sensitivity analysis on influencing factors

C. Yoo & E.M. Jung

Sungkyunkwan University, Suwon, Korea

**ABSTRACT:** This paper concerns a sensitivity analysis on influencing factors which affect tunnelling induced ground surface settlements in groundwater drawdown environment. A Seoul metro extension design project, in which ground settlements associated tunnelling-induced groundwater drawdown was a key design issue, was selected to identify governing mechanisms and influencing factors. A series of two-dimensional finite element analysis were performed on a number of conditions encountered in the project to form a database with due consideration of the tunnelling and groundwater interaction. The results of the parametric study were then analyzed so as to relate the influencing factors to the ground surface settlement development. Practical implications and findings of the study are discussed

### 1 INTRODUCTION

Tunnel construction inevitably results in groundwater inflow into the excavated area when tunnelling under the groundwater table, thus causing the groundwater drawdown. Such a tunnelling-induced groundwater drawdown induces associated settlements in addition to the settlement due to the excavation (Yoo 2005; Yoo and Kim 2006). The related ground subsidence occurring as a result of the reduction in water pressures in the soil layers can damage nearby structures/utilities.

Recently, there have been a number of case histories in which the development of excessive settlements during tunnelling in groundwater drawdown environment have become serious construction issues. One of the recent case histories is the excessive settlement during construction of tunnels under an apron area of a domestic airport in Seoul. The NATM tunneling in water bearing permeable ground caused excessive surface settlements on the airport apron and therefore serviceability issues of nearby facilities were raised.

As seen in Fig. 1, excessive surface settlements up to 160 mm occurred over a 100 m zone within the airport apron as shown in Fig. 1. Serviceability issue of the airport facility became an issue causing serious construction problem.

In this paper the results of a parametric study on groundwater drawdown induced surface settlement during an urban tunnelling situation. A Seoul metro extension design project, in which ground settlements associated tunnelling-induced groundwater drawdown was a key design issue, was selected for the parametric study to represent a more realistic tunnelling condition. Using a calibrated stress-pore pressure coupled finite element model which can simulate the tunnelling and groundwater interaction, a parametric analysis was performed on a number of conditions encountered in

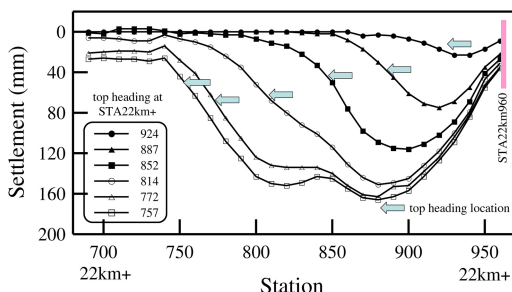


Figure 1. A case history of excessive settlement (after Yoo et al. 2012).

the project to form a database. The results of the parametric study are then analyzed to investigate the influencing factors on the ground surface settlement development.

### 2 TUNNELLING DESIGN PROJECT CONSIDERED

#### 2.1 Project site

Fig. 2 shows the longitudinal tunnel alignment is shown. The tunnel at the site has a diameter of 10 m with cover depths ranging 15~40 m over a length of 5.6 km under heavily populated urban environments. The cross section of the excavation area, shown in Table 1, ranges approximately 100~120 m<sup>2</sup> and the drill and blast method is adopted as the primary excavation method. The ground at the site consists of a 5 to 20 m thick layer of miscellaneous fill material including sand, gravel, and silty clay. Underlying the fill layer is a 5 to 20 m thick decomposed granitic rock

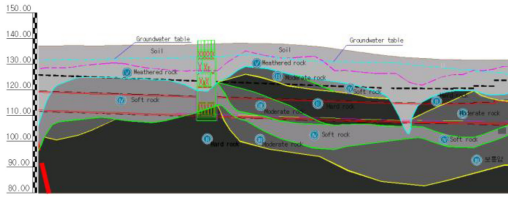


Figure 2. Longitudinal tunnel alignment.

Table 1. Geotechnical properties of ground layers.

Ground	$E^{1)}$ (MPa)	$\nu^{2)}$	$c^{3)}$ (kPa)	$\phi^{4)}$ (deg)	$k^{5)}$ (cm/s)
Fill	20	0.3	21	29	$2.7 \times 10^{-3}$
WR <sup>67)</sup>	290	0.3	70	32	$6.2 \times 10^{-4}$
SR <sup>7)</sup>	910	0.27	440	37	$2.9 \times 10^{-5}$
MR <sup>8)</sup>	4,000	0.25	1,200	40	$1.4 \times 10^{-5}$
HR <sup>9)</sup>	10,250	0.23	2,300	42	$6.6 \times 10^{-5}$

<sup>1)</sup>  $E$  = elastic modulus; <sup>2)</sup>  $\nu$  = Poisson's ratio; <sup>3)</sup>  $c$  = cohesion; <sup>4)</sup>  $\phi$  = internal friction angle; <sup>5)</sup>  $k$  = hydraulic conductivity; WR = weathered rock; SR = soft rock; MR = medium rock; HR = hard rock

layer underlain by a 10 to 20 m thick solid granitic rock layer. Below the weathered granite rock layer is a soft to hard granitic rock layer. The ground along the tunnel route was classified into four general types of Class II to V based on the RMR classification. The engineering properties of the rock and soil layers are given in Table 1.

## 2.2 Tunnel section

The project site involves a tunnel section having a width and height of approximately 10.5 m and 8.7 m, respectively, with a cover depth ranging approximately 20~30 m. Although now shown, the primary support system consisted of a 0.25~0.15 m thick steel fibre reinforced shotcrete (SFRS) layer with 4 m long system rock bolts at (0.8~1.0) m and (1.0~1.2) m, respectively, longitudinal and transverse spacing. The pipe umbrella technique using 800 mm diameter grout injected 12 m long steel pipes are additionally adopted for PD-2B to promote the face stability through improving the load carrying capacity of the ground ahead of the face. For the remaining support patterns, the fore poling is used when necessary. No pre or post grouting is adopted, although the groundwater level is quite high at the ground level (GL) – 3 m.

## 3 TWO-DIMENSIONAL STRESS-PORE PRESSURE COUPLED FINITE ELEMENT ANALYSIS

### 3.1 Tunneling condition considered

A 2D stress-pore pressure coupled finite element model was adopted in the parametric study on the

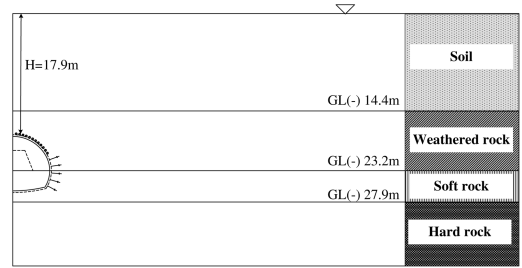


Figure 3. Tunneling condition considered.

Table 2. Parameter ranges considered.

Thickness of soil layer (m)	$k$ (m/day)	$E$ (MPa)	$e_o^{1)}$ (MPa)	$k_{shot}^{2)}$ (cm/s)
0~15	1.6~2.6	20~70	0.7~1.4	0.02~0.0002

<sup>1)</sup>  $e_o$  = initial void ratio; <sup>2)</sup>  $k_{shot}$  = hydraulic conductivity of shotcrete lining

tunnelling condition, given in Fig. 3, considering the project site shown in Fig. 2 aiming at identifying influencing factors governing the groundwater drawdown induced settlement during tunnelling.

A number of cases were first developed for the support patterns by varying the influencing factors as summarized in Table 3. The developed cases were then analyzed assuming the tunnel section reaching a plane strain section in 20 days, i.e., 1.5 m/day advance rate. Note that the 1.5 m/day advanced rate considered represents the tunnelling practices in Korea, and that the range of each parameter represents typical tunnelling cases in Korea.

### 3.2 Stress-pore pressure coupled finite element

The commercially available finite-element package Abaqus 6.11 (Abaqus 2011) was used for analysis which is capable of simulating the stress-strain-strength behavior of ground in stress-pore pressure fully coupled manner. Note that the importance of carrying out the stress-pore pressure fully coupled analysis for tunnelling cases where the interaction between the tunneling and groundwater takes place has been discussed by Yoo (2005).

A porous medium is modeled approximately in ABAQUS by attaching the finite element mesh to the solid phase. A continuity equation, equating the rate of increase in liquid mass stored at a point to the rate of mass of liquid flowing into the point within the time increment, is written in a variational form as a basis for finite element approximation as Eq. (1).

$$\int \sigma : \delta \epsilon dV = \int t \cdot \delta v dS + \int \hat{f} \cdot \delta v dV \quad (1)$$

where  $dv$  is a virtual velocity field,  $\delta\varepsilon = \text{sym}(\partial\delta v/\partial x)$  is the virtual rate of deformation,  $\sigma$  is the true (Cauchy) stress,  $t$  are surface tractions per unit area, and  $\hat{f}$  body forces per unit volume. For coupled analysis,  $\hat{f}$  includes the weight of the wetting liquid.

$$\hat{f}_w = (sn + n_t)\rho_w g \quad (2)$$

where  $\rho_w$  is the density of the wetting liquid and  $g$  is the gravitational acceleration, which we assume to be constant and in a constant direction. Considering this loading explicitly so that any other gravitational term in  $\hat{f}$  is associated only with the weight of the dry porous medium. Equation (1) can be rewritten as Eq. (3):

$$\int_V \sigma : \delta\varepsilon dV = \int_S t \cdot \delta v dS + \int_V f \cdot \delta v dV + \int_V (sn + n_t)\rho_w g \cdot \delta v dV \quad (3)$$

where  $f$  are all body forces except the weight of the wetting liquid. The liquid flow is described by introducing Darcy's law or, alternatively, Forchheimer's law.

The continuity equation is satisfied approximately in the finite element model by using excess wetting liquid pressure as the nodal variable (degree of freedom 8), interpolated over the elements. The equation is integrated in time by using the backward Euler approximation. The total derivative of this integrated variational statement of continuity with respect to the nodal variables is required for the Newton iterations used to solve the nonlinear, coupled, equilibrium and continuity equations.

### 3.3 Finite element model

A typical the finite element model adopted in this study is shown in Figure 5. Taking advantage of the symmetry about the tunnel centerline, only half of the tunnel section was modeled. As seen, the finite-element mesh extends to the solid rock layer and laterally to a distance of  $18D$  from tunnel central axis. At the vertical boundaries, displacements perpendicular to the boundaries are restrained whereas pin supports were applied to the bottom boundary.

With regard to the hydraulic boundary conditions and with reference to Figure 4, a no-flow condition was assigned to the left vertical boundary while a constant hydraulic water pressure assuming the groundwater level at GL-3m was assumed throughout the analysis. The locations of the lateral and bottom boundaries were selected so that the presence of the artificial boundaries does not significantly influence the stress-strain-pore pressure field in the domain. Free drainage was allowed at the excavated surface by assigning zero pore pressure flow boundary condition to allow for the water inflow to occur during tunnel excavation.

In the discretization 8-node displacement and pore pressure elements with reduced integration (CPE8RP) were used for the soil/rock layers below the initial groundwater table, and the shotcrete lining while the

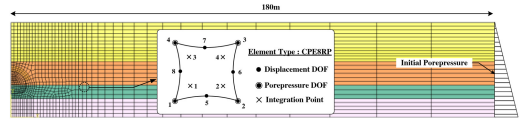


Figure 4. Finite element model adopted.

soil layer above the groundwater table was discretized using 8 node stress/displacement elements (CPE8RP). The soil and rock layers were assumed to be an elastoplastic material conforming to the Mohr-Coulomb failure criterion together with the non-associated flow rule proposed by Davis (1968), while the shotcrete lining was assumed to behave in a linear elastic manner. The time dependency of the strength and stiffness of the shotcrete lining after installation was not modelled in the analysis, but rather an average value of Young's modulus of 10 GPa representing green and hard shotcrete conditions reported in literature (Queiroz et al. 2006) was employed.

The 3D effects of advancing a tunnel heading was accounted for by using the "stress relaxation method" in which the boundary stresses arising from the removal of excavated elements are progressively applied to simulate the progressive release of the excavation forces as the tunnel heading advances. Modeling the 3D effects using a 2D model for a tunneling problem is beyond the scope of study and can be found elsewhere (Bernat and Cambou 1995; Yoo et al. 2007).

## 4 RESULTS OF SENSITIVITY ANALYSIS

The relative importance of the factors considered in this study on the maximum surface settlement ( $S_{v,max}$ ) was investigated using the results of the parametric study. The variations of  $S_{v,max}$  with the thickness of soil layer within the drawdown zone ( $H_{d,s}$ ) and the shotcrete lining permeability coefficient ( $k_{shot}$ ) are shown in Fig. 5. Note that  $k_{shot}$  is in fact indirectly related to the groundwater inflow into the tunnel. As seen, despite of the scatter in the data shown in Fig. 5(a), the trend of increasing  $S_{v,max}$  with increasing  $H_{d,s}$  for a given tunnelling condition is evident such that the larger the  $H_{d,s}$ , the greater is the  $S_{v,max}$ . In addition, for a given  $H_{d,s}$ , it can be seen in Fig. 5(b) that the settlement  $S_{v,max}$  increases with increasing the shotcrete lining permeability  $k_{shot}$  due to large water inflow into the tunnel when  $k_{shot}$  is larger. The variation of  $S_{v,max}$  with  $k_{shot}$  is however greater when the thickness of soil layer within the drawdown zone  $H_{d,s}$  is larger.

Fig. 6 illustrates the variations of  $S_{v,max}$  with geotechnical parameters of the soil layer within the groundwater drawdown zone. According to the results in these figures, the primary influencing factors appears to be the stiffness of the soil layer  $E$  while the initial void ratio  $e_o$  and the permeability  $k_s$  being the secondary influencing factors. For example, as shown

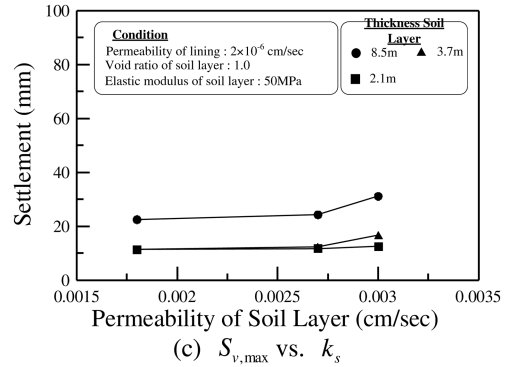
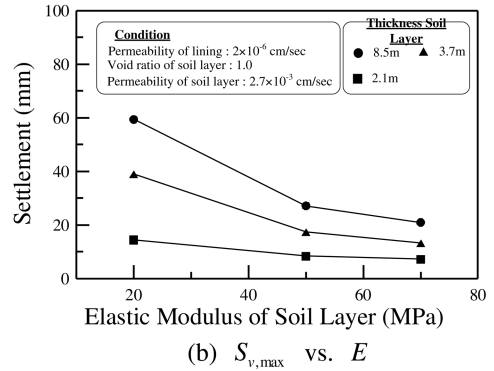
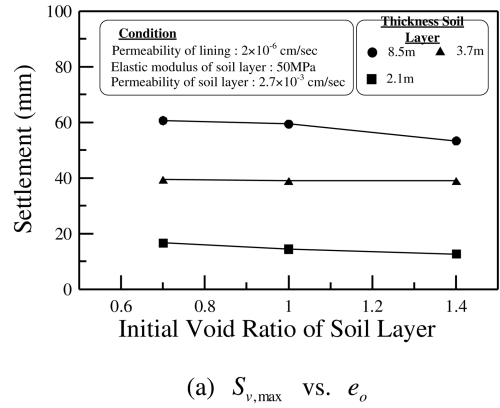
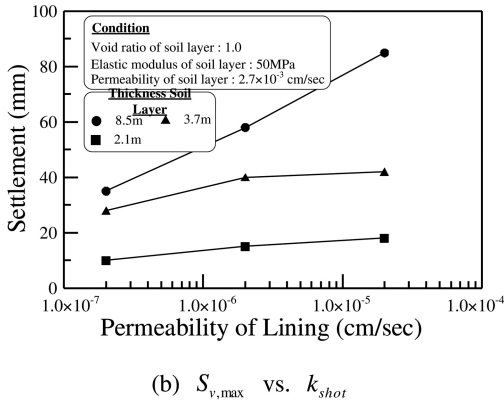
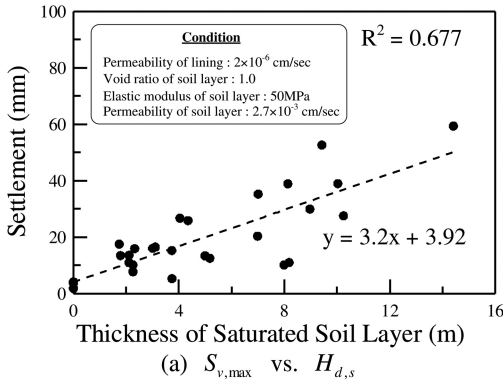


Figure 5. Variations of maximum surface settlement  $S_{v,max}$  with  $H_{d,s}$  and  $k_{shot}$ .

in Fig. 6(a), the variance of  $S_{v,max}$  with the range of  $e_o$  and  $k_s$  considered is 15% at the maximum for the range of  $H_{d,s} = (2 \sim 8.5)$  m. The variation of  $S_{v,max}$  with the stiffness of the soil layer  $E$  is more dramatic showing the variation of 50% for the range of  $E$  considered.

## 5 CONCLUSIONS

In this paper, the results of a parametric study on groundwater drawdown induced surface settlement during an urban tunnelling situation are presented. A Seoul metro extension design project, in which ground settlements associated tunnelling-induced groundwater drawdown was a key design issue, was selected for the parametric study to represent a more realistic tunnelling condition. Using a calibrated stress-pore pressure coupled finite element model which can simulate the tunnelling and groundwater interaction, a parametric analysis was performed on a number of condition encountered in the project to form a database

It is shown that the groundwater drawdown during tunnelling causes increases in the effective stress in the drawdown affected area due to the pore pressure reduction caused by the drawdown. The resulting reduction in the void ratio causes additional settlement in addition to the settlement by the unloading effect due to tunnel excavation. The results also indicated that the primary influencing factors on the settlement

Figure 6. Variations of maximum surface settlement  $S_{v,max}$  with  $e_o$ ,  $E$ , and  $k_s$ .

development are the thickness and stiffness of soil layer within the drawdown zone, and the shotcrete lining permeability while the initial void ratio together with the permeability of the soil layer within the drawdown zone are secondary influencing factors.

## ACKNOWLEDGEMENT

This research is supported by Grant No. 10CCTI-E09 and 13CCTI-T01 from the Ministry of Land, Transport

and Maritime Affairs, Korea. The financial support is gratefully acknowledged.

## REFERENCES

- Abaqus, Inc. 2011. ABAQUS user's manual, version 6.11. Abaqus, Inc., Pawtucket, Providence, R.I.
- Bernat, S. and Cambou, B. Modeling of tunnel excavation in soft soil. Proc. 5th symposium on Numerical Models in Geomechanics. 1995; 1: 471–476.
- Davis, E. H. 1968. Theories of plasticity and the failure of soil masses. Soil mechanics: Selected topics, Butterworth's London, U.K. 341–380.
- Queiroz, P.I.B., Roure, R.N., and Negro, A. 2006. Bayesian updating of tunnel performance for  $K_o$  estimate of Santiago gravel. In Proceedings of the International Symposium on Geotechnical Aspects of Underground Construction in Soft Ground, London, 15–17 June. Taylor and Francis/Balkema, Leiden, The Netherlands. 211–217.
- Yoo, C. 2005. Interaction between Tunnelling and Groundwater-Numerical Investigation Using Three Dimensional Stress-Pore Pressure Coupled Analysis. *Journal of Geotechnical and Geoenvironmental Engineering, ASCE*, 131(2): 240–250.
- Yoo, C. & Kim, S.B. 2006. Stability analysis of an urban tunnelling in difficult ground condition. *Tunnelling and Underground Space Technology, Elsevier* 21(3–4): 351–352.
- Yoo, C., Lee, Y.J., Kim, S.H. & Kim, H.T. 2012). Tunnelling-induced ground settlements in a groundwater drawdown environment – A case history. *Tunnelling and Underground Space Technology, Elsevier* 29(3): 69–77.